# Chapter 3

# Optimal design of DC-DC converter for MPPT applications

## 3.1 Introduction

This chapter presents the design optimization of a non-isolated DC-DC boost converter. The steady state model of the converter along with the mathematical model for design optimization is presented. The optimized boost converter for MPPT applications in standalone PV systems is also investigated. Finally, the optimally designed converter is implemented to track the MPP using existing tracking algorithms for different scenarios of irradiance and temperature profile.

## 3.2 Steady State Space Model of DC-DC Boost Converter

The DC-DC boost converter offers great tracking efficiency in challenging conditions when used in photovoltaic (PV) systems for peak power point tracking [209]. A dc-dc converter's design optimization aims to lower the total power loss across the different switch operation stages in the MOSFET. The parameters considered in this study for the design optimization includes the sizing of inductor, capacitor, switching frequency and the bounds of constraints that takes into consideration the continuous conduction mode (CCM) of operation, continuous voltage mode (CVM) of operation, bandwidth (BW) and ripple content in output current and voltage. The DC-DC boost converter's optimal design is considered as a single op-

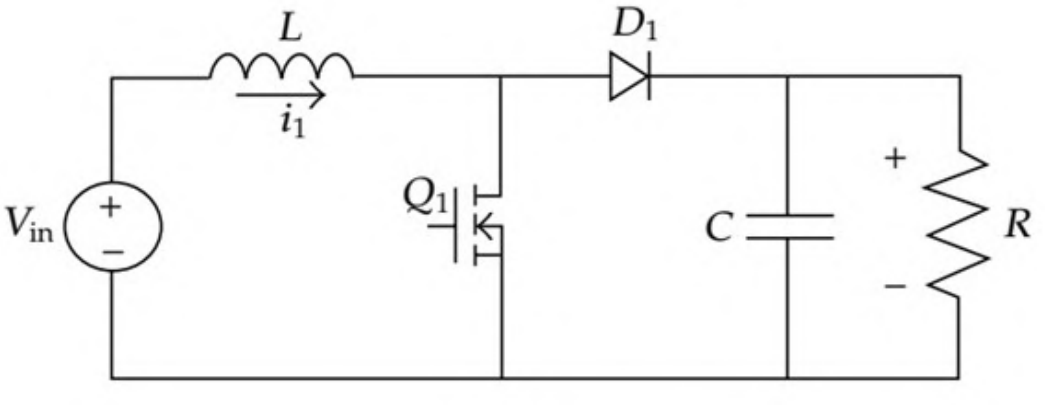


**Figure. 3.1:** Electrical circuit of a DC-DC Boost Converter

timization problem. The electrical circuit of the DC-DC boost converter is shown in figure 3.1. The governing equations in the modeling using the state vector approach is given by [196, 244]:

$$x = \begin{bmatrix} i_1 \\ v_o \end{bmatrix} \tag{3.1}$$

$$\frac{di_1}{dt} = -\frac{v_o}{L}(1-u) + \frac{V_{in}}{L}u \tag{3.2}$$

$$\frac{dv_o}{dt} = \frac{i_c}{C}(1-u) - \frac{V_C}{RC} \tag{3.3}$$

Where, $i_1$ in equation (3.1) represents the current flowing in the inductor and the output voltage is given by $v_o$ . The switch state is represented by the parameter u in equation (3.2) and (3.3) where the ON state (u=1) (under this condition the $Q_1$ is ON and $D_1$ is inactive) and OFF state (u=0) (under this condition $Q_1$ is OFF and $D_1$ is active) determine the operation of the switching device. The initial value of u functions as the control signal to regulate how the converter operates. The circuit parameters representing the inductor, capacitor, input voltage and load resistance are denoted by L, C, $V_{in}$ and R respectively. The current and voltage ripples along with the dimension of the inductor for the CCM operation and the BW limitation impose the constraints to the optimization problem. They are calculated as:

$$\Delta i_1 = \frac{V_{in}D}{Lf_s} \tag{3.4}$$

$$\Delta v_o = \frac{V_C D}{f_s C R} \tag{3.5}$$

$$L f_s = \frac{V_C}{2 I_o} D(1-D)^2 \tag{3.6}$$

$$\omega_o = \frac{(1-D)}{\sqrt{LC}} \tag{3.7}$$

$$\omega_o > 2\pi(a f_s) \tag{3.8}$$

Where the switching frequency is given by $f_s = \frac{1}{T_s}$, $T_s$ being the switching period and $f_s$ the switching frequency, and a is a percentage of $f_s$. The total power loss calculations depend on the losses incurred during the converter's operation as well as any losses brought on by parasitic resistance loss and parasitic capacitance-induced switching losses. In addition, the device operation loss due to the ON-OFF state transitions at the conclusion of each cycle also effect the power calculation and hence the efficiency of the converter. The total power loss taking place in one complete cycle of operation of the boost converter denoted by $P_{BOOST}$ is given by:

$$P_{Q1} = P_{ON} + P_{SW} \tag{3.9}$$

$$P_{ON} = \left( (\frac{I_o}{1-D})^2 + \frac{\Delta i_1^2}{12} \right) D R_{DS} \tag{3.10}$$

$$\begin{aligned} P_{SW} = (V_C - V_f) \left( (\frac{I_o}{1-D}) - \frac{\Delta i_1}{2} \right) T_{swon} f_s \\ +(V_C - V_f) \left( (\frac{I_o}{1-D}) + \frac{\Delta i_1}{2} \right) T_{swoff} f_s \end{aligned} \tag{3.11}$$

$$P_d = V_f I_o (1-D) + Q_{rr}^{Schotty} V_c f_s \tag{3.12}$$

$$P_{ind} = \left( (\frac{I_o}{1-D})^2 + \frac{\Delta i_1^2}{12} \right) R_L \tag{3.13}$$

$$P_{cond} = I_{effc}^2 R_C \tag{3.14}$$

$$P_{BOOST} = P_{Q1} + P_d + P_{ind} + P_{cond} \tag{3.15}$$

The effectiveness of a converter is determined by:

$$\eta = \frac{P_{LOAD}}{P_{LOAD} + P_{BOOST}} \times 100 \tag{3.16}$$

$P_{LOAD}$ represents the output power of the converter. While the ON time and the OFF time for the converter is represented by $T_{swon}$ and $T_{swoff}$ respectively. $I_o$ gives average output current, while $R_{DS}$ provides the MOSFET's on-state resistance. The inductor's loss component is represented by $R_L$ and the corresponding series resistance is shown for the capacitor by $R_C$.

## 3.3 Mathematical formulation of the Design optimization Problem

Optimal selections of converter design parameters, i.e., to set up the optimization problem, operational constraints are to be be taken into consideration while defining the objective function. The current problem at hand encompasses solving the optimization problem to achieve minimized operational losses in the DC-DC converter, or for $P_{BOOST}$ to be minimal. The constraints considered in the optimization problem are the constraints on the design variables maximum and minimum values, the ripple constraints, the CCM operation criterion as per Equations (3.4)-(3.5), and the BW constraint as per Equation (3.8) for the boost converter. The mathematical representation of minimizing $P_{BOOST}$ has the following constraints as:

$$L_{min} \leq L \leq L_{max} \tag{3.17}$$

$$C_{min} \leq C \leq C_{max} \tag{3.18}$$

$$f_{smin} \leq f_s \leq f_{smax} \tag{3.19}$$

$$\Delta i_1 < a\% I_o \tag{3.20}$$

$$\Delta v_C < b\% V_C \tag{3.21}$$

Here a and b in equations (3.20) and (3.21) are the limits on the percentage averaged magnitude of current and voltage, and which act as the ripple constraints for current and voltage for the converter.

## 3.4 Design optimization of DC-DC Boost converter

Metaheuristics have been successfully employed to solve the harmonics in multilevel inverters [246, 266]. The authors in the work note that in order to make a comparative assessment of algorithms, they must be evaluated against similar performance metrics. They utilized the iteration time, convergence characteristics and statistical parameters to map the performance of the selected algorithms. In this study, the same procedure is adopted to make a comparison of the optimization algorithms to ascertain peak performance. To ensure attainment of global optima, the work in this chapter presents the design of optimized DC-DC converter operating at minimum operational loss utilizing twenty-three metaheuristic algorithms. The problem formulation philosophy indicating the state space modeling for optimal selection of design parameters for the DC-DC boost converter has already been discussed in section 3.2 along with the formulation of design optimization problem (in section 3.3). The simulation of results are covered in detail followed by section 3.6 with the discussion of pertinent results.

Table 3.1 presents the list of the twenty-three optimization algorithms' control settings. In this study, we ensure optimal performance for each algorithm by utilizing the suggested parameter combinations from the source literature as reported previously in Chapter 2, section 2.2. The algorithms' population size is set at 30, while there can be a maximum of 100 iterations. To acquire statistical findings, each algorithm in the current study is run for a 100 iterations, and for each technique, the optimum fitness function value is reported. The simulation experiments are conducted on a computer system with an Intel Core i7 CPU, 16 GB RAM, and running on Windows 10. For the optimal design of the converter the constraints and the range of the design parameters are given in table 3.2. The range of the design parameters have been considered from the reported research work presented in [202]. It is important to note that variations in the these values in a DC-DC boost converter significantly affect performance metrics, including current ripple, output voltage ripple, efficiency, and transient response [54, 161]. Decreasing the inductance results in increased current ripple and may transition the converter into discontinuous conduction mode (DCM). Conversely, increasing L diminishes ripple but leads to larger size and slower transient response. Smaller capacitance (C) leads to increased output voltage ripple, while larger capacitance enhances filtering but may elevate costs and diminish dynamic performance. The optimal selection of inductance (L) and capacitance (C) necessitates a careful

**Table 3.1:** Parameters defined for the optimization algorithms in the current study

| Optimization Algorithm | Parameter | Selected parameter value |
|---|---|---|
| ABC | Modification rate | 0.8 |
| AHA | Migration Co-efficient | 2n,n = 30 |
| ALO | Number of Ant-Lions, Selection Method | 30, Roulette Wheel |
| DFA | Enemy factor, Separation weight, alignment weight, cohesion weight, food factor | Decreases linearly from 0.1 to 0,[0,0.2] and [0,1] |
| FFA | Randomness index, absorption coefficient, beta | 0.25, 1, 0.20 |
| GWO | Convergence parameter a, random variables r1, r2 | Linearly decreased from 2 to 0, [0,1] |
| IGWO | Convergence parameter a, random variables r1,r2 | Linearly decreased from 2 to 0, [0,1] |
| HHO | Escaping energy of prey E, chance of escapes r | [-1,1] and [0,1] |
| MFO | Convergence constant r, spiral constant b | Decreases linearly from -1 to -2, 1 |
| MPA | Constant P, probability of fish aggregating devices effect | 0.5, 0.2 |
| PSO | Weight factor w, constants c1 and c2 | w = 1, c1 = c2 = 2 |
| SCA | Convergence factor r1, , random numbers r2, r3 and r4. | Decreases linearly from 2 to 0, 0 to $2\pi$, 0 to 2 and 0 to 1. |
| SSA | Controlling parameter c1, random variables c2 , c3 | Decreases exponentially through 2 to 0, [0,1] |
| WOA | Convergence parameter | Decreases linearly from 2 to zero |
| AEFA | Coulomb constant K0, learning rate $\alpha$ | 500, 30 |
| ASO | Depth weight $\alpha$ , multiplier weight | 50, 0.2 |
| BB-BC | Parameter for controlling the influence center of mass (CM) and best particle, alpha | 0.2, |
| EO | Generation Probability, exploitation ability control and management constant a1, a2. | 0.5, 2,1 |
| FDA | Alpha , Beta | 30, 1 |
| MVO | Wormhole existence probability min and max | 0.2, 1 |
| AOA | Math optimizer probability, Sensitivity parameter, Control parameter | [0.2, 1], 5, 0.5 |
| GA | Type, selection , crossover, mutation rate | Real coded Roulette Wheel, Crossover Probability 0.8, Gaussian 0.05 |
| TLBO | Teaching Factor | [1,2] |

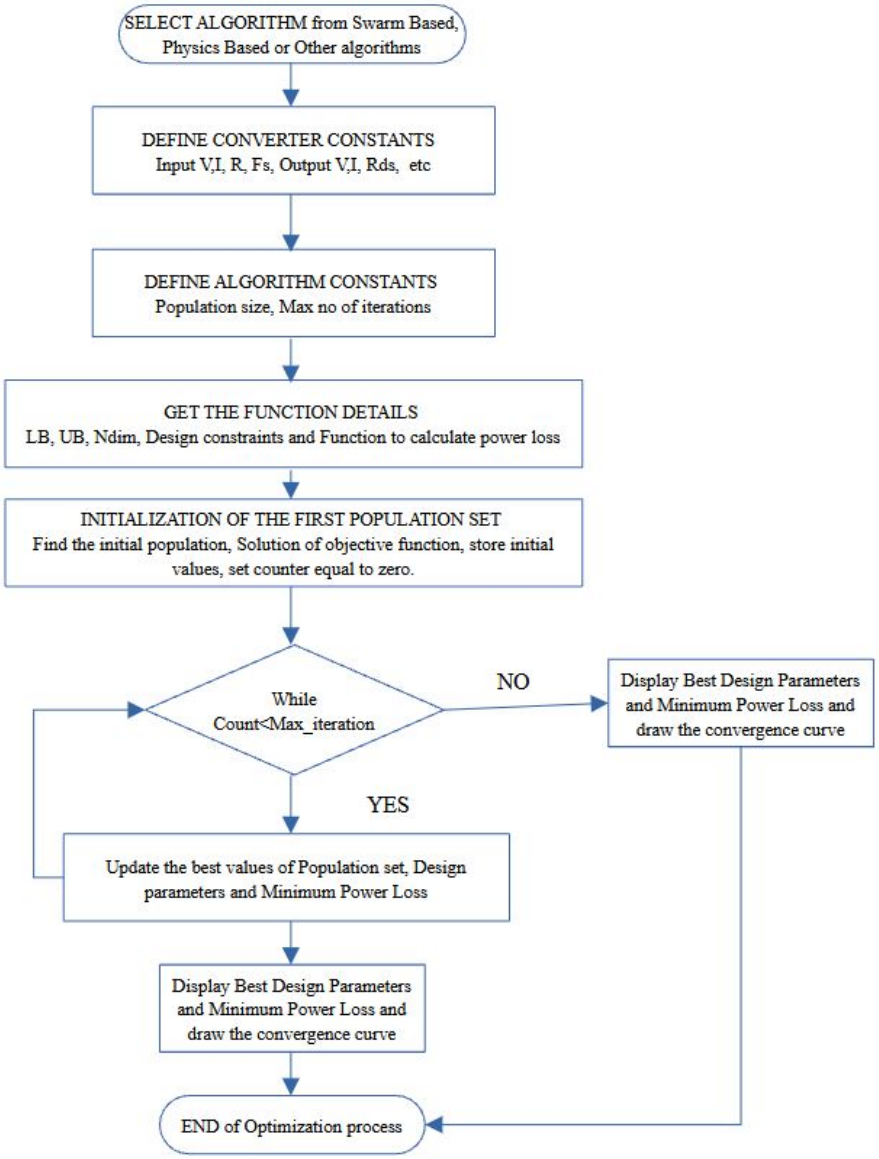


**Figure. 3.2:** Overall flowchart for the workflow of optimization of DC-DC converters using metaheuristic algorithms

balance of trade-offs among size, efficiency, and performance.

The flowchart in figure 3.2 shows the overall scheme of the methodology followed for the optimal design of the individual converters. The findings for each algorithm are shown in Tables 3.3 for the minimized converter power loss for boost converter. Table 3.4 presents the final values of the design constraints for the optimization problem, aimed at minimizing power loss in the boost converter ($P_{boost}$). In the specified range presented in table 3.2, the decision variables for the optimization problem include inductance (L), capacitance (C), and frequency (Fs). The minimum value of $P_{boost}$ determined by the algorithm during the optimization process will depend on the optimal combination of L, C, and Fs values within

the specified range presented in table 3.2. The variations stem from the unique search mechanisms utilized by each optimization algorithm, which, despite differing methodologies, effectively identify parameter combinations that meet design constraints while achieving the minimum power loss. To achieve the minimum value of $P_{boost}$, the variations in L and C values across different optimization algorithms indicate the presence of multiple viable solutions.

**Table 3.2:** Design parameters and constraints as inputs considered for optimization of DC-DC boost converter [202]

| Parameter | Value | Parameter | Value |
|---|---|---|---|
| Inductor values | (0.1µH–10 mH) | Output Voltage | 10V |
| Capacitor values | (0.1µF–100µF) | Input Voltage | 5V |
| Switching frequency Values | (10kHz-800kHz) | Output Current | 2A |
| On state resistance | 5.2 mΩ | Converter On time | $10^{-8}$s |
| Reverse Recovery Charge | 50 x $10^{-9}$ A | Converter Off time | $10^{-8}$s |
| a | 15% of $I_o$ | Forward Voltage Drop | 0.9 V |
| b | 15% of $V_C$ | | |

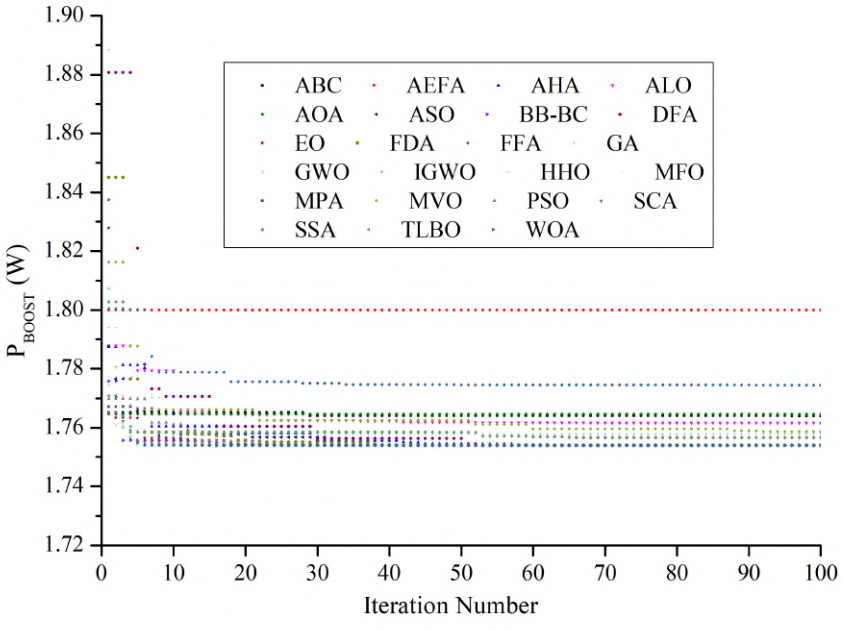


**Figure. 3.3:** Convergence characteristics for the Boost Converter

Table 3.3 and figure 3.3 show that the GWO, MFO, PSO, SCA, SSA, WOA, AOA and GA produce the favorable results in terms of iteration time for the boost converter design optimization, with GA taking the least iteration time

**Table 3.3:** Statistical parameters for the optimal design of the boost converter

| Optimization Algorithm | Best (W) | Mean Value(W) | Worst Value(W) | Standard Deviation | Iteration time (s) |
|---|---|---|---|---|---|
| ABC | 1.75659 | 1.76428 | 1.76507 | 8.92E-4 | 0.924952 |
| AHA | 1.7539 | 1.7573 | 1.78751 | 0.00701 | 0.92 |
| ALO | 1.76158 | 1.76428 | 1.78782 | 0.0064 | 14.6096 |
| DFA | 1.75388 | 1.76292 | 1.88074 | 0.02561 | 166.3101 |
| FFA | 1.77443 | 1.77673 | 1.80042 | 0.00619 | 4.423415 |
| GWO | 1.75389 | 1.75433 | 1.7746 | 0.00233 | 0.685787 |
| IGWO | 1.75388 | 1.7548 | 1.80727 | 0.00597 | 8.52949 |
| HHO | 1.75388 | 1.75551 | 1.79399 | 0.00603 | 1.55345 |
| MFO | 1.75388 | 1.75565 | 1.77729 | 0.00567 | 0.76824 |
| MPA | 1.75388 | 1.75507 | 1.76714 | 0.00333 | 2.1815 |
| PSO | 1.75388 | 1.75548 | 1.76988 | 0.00408 | 0.612471 |
| SCA | 1.75389 | 1.75443 | 1.76507 | 0.00184 | 0.620821 |
| SSA | 1.75659 | 1.75894 | 1.80274 | 0.00775 | 0.459486 |
| WOA | 1.75403 | 1.75519 | 1.83733 | 0.00856 | 0.373068 |
| AEFA | 1.79986 | 1.79986 | 1.79986 | 0 | 2.811 |
| ASO | 1.75393 | 1.75634 | 1.78768 | 0.00564 | 7.984897 |
| BB-BC | 1.75389 | 1.75462 | 1.77576 | 0.00308 | 0.924952 |
| EO | 1.75388 | 1.75519 | 1.82784 | 0.00759 | 1.628476 |
| FDA | 1.75388 | 1.75786 | 1.84504 | 0.01577 | 2.08656 |
| MVO | 1.75862 | 1.76373 | 1.81616 | 0.01025 | 0.93446 |
| AOA | 1.75465 | 1.76925 | 1.80798 | 0.01159 | 0.57074 |
| GA | 1.75388 | 1.7544 | 1.77074 | 0.00263 | 0.369388 |
| TLBO | 1.75659 | 1.76003 | 1.88836 | 0.01333 | 1.648833 |

to execute the optimization problem. The GWO and WOA perform better than any other swarm intelligence-based algorithms when measured against the convergence curve. The two algorithms produced better results with the best cost function values (the smallest power loss in the converter), mean values, and standard deviation, demonstrating its superiority in the swarm intelligence category of algorithms. If we take into account Physics-Based algorithms and other algorithms in the same way, we discover that the BB-BC and GA, respectively, are the superior algorithms in each category in terms of least iteration time and smallest standard deviation.

The SSA and MFO perform better than any other swarm intelligence-based algorithms when measured against the convergence curve. The WOA algorithm exhibits its dominance across the swarm intelligence category of algorithms for the optimized values for cost function (the minimum power loss in the converter). Mean values and standard deviation also showed enhanced outcomes produced by the iteration process for the WOA algorithm. If we look at Physics-Based

**Table 3.4:** Optimal value of the design parameters for the Boost converter

| Optimization Algorithm | L (mH) | C ($\mu$F) | Fs (kHz) | $P_{BOOST}$(W) | $\eta$(%) |
|---|---|---|---|---|---|
| ABC | 9.31 | 79.97 | 157.73 | 1.7643 | 91.89 |
| AHA | 7.53 | 99.79 | 100.37 | 1.7573 | 91.92 |
| ALO | 5.73 | 81.94 | 127.95 | 1.7643 | 91.89 |
| DFA | 7.551 | 95.93 | 105.74 | 1.7629 | 91.89 |
| FFA | 5.16 | 64.75 | 158.32 | 1.7767 | 91.84 |
| GWO | 6.16 | 99.99 | 100.02 | 1.7543 | 91.93 |
| IGWO | 10 | 100 | 100.00 | 1.7548 | 91.93 |
| HHO | 9.98 | 99.99 | 100.02 | 1.7555 | 91.93 |
| MFO | 9.98 | 99.97 | 100.04 | 1.7556 | 91.93 |
| MPA | 10 | 100 | 100.00 | 1.7551 | 91.93 |
| PSO | 10 | 100 | 100.00 | 1.7555 | 91.93 |
| SCA | 7.3 | 100 | 100.28 | 1.7544 | 91.93 |
| SSA | 5.76 | 84.63 | 122.01 | 1.7589 | 91.92 |
| WOA | 8.29 | 97.70 | 109.65 | 1.7552 | 91.93 |
| AEFA | 4.72 | 65.65 | 520.01 | 1.7998 | 91.74 |
| ASO | 5.03 | 83.39 | 125.84 | 1.7563 | 91.93 |
| BB-BC | 10 | 100 | 100.14 | 1.7546 | 91.93 |
| EO | 9.87 | 99.99 | 100 | 1.7552 | 91.93 |
| FDA | 9.99 | 100 | 100 | 1.7578 | 91.92 |
| MVO | 9.95 | 91.60 | 110.73 | 1.7637 | 91.89 |
| AOA | 4.38 | 64.39 | 224.74 | 1.7693 | 91.87 |
| GA | 6.98 | 94.88 | 129.32 | 1.7600 | 91.91 |
| TLBO | 10 | 100 | 100 | 1.7544 | 91.93 |

algorithms, BB-BC and MVO have convergence characteristics that are quite comparable, but MVO performs better in terms of iteration time, best value, minimum value, and smallest standard deviation than the other algorithms. In the category of other algorithms, AOA and GA, respectively, are quite comparable in terms of minimal iteration time and minimal standard deviation. However, GA provides a better value for the cost function, iteration time, and standard deviation proving its superiority over AOA and TLBO.

From the results, it is observed that when taking into account the standard deviation and iteration time as the performance criterion, WHO within the swarm intelligence based category gives superior results (table 3.3 and table 3.4). If comparison of WHO is made with respect to other algorithms within the swarm intelligence category, the results indicate that WHO also solves the total power loss reduction issue with a quick convergence rate. With the exception of ALO and FFA, which give the optimal solutions corresponding to 1.764 and 1.776 W, respectively, practically all approaches achieve the optimized value of 1.754 W.

When comparing the standard deviation values and percentage efficiency of the optimization approaches in the category of physics-based methods in reported in Table 3.3 and 3.4, it becomes clear that the BB-BC is more reliable and efficient than all the other methods for resolving the current design optimization problem for least amount of power loss. Furthermore, from the convergence rate comparison (figure 3.3) it is observed that BB-BC and EO converge considerably more quickly than other algorithms in this category. Thus, the BB-BC approach provides the superior optimal solutions in this group. The TLBO, AOA, and GA methods also achieve the optimal value of 1.75 W. When taking into account figure 3.3 and Table 3.3 and Table 3.4, GA gives improved performance for minimizing power loss and accelerating convergence. The approach is also more reliable due to its low standard deviation value.

Figure 3.3 shows how well the 23 reference optimization strategies obtain the least amount of power loss for the optimally designed parameters. The overlap of graphs take place because the outcomes are similar. The results have therefore been assessed in light of the optimized results as well as the converter design parameters for the filter inductor, filter capacitor, switching frequency, standard deviation, best, mean, and average values provided by table 3.3.The CCM and BW constraints are two of the most significant design requirements that must be addressed while choosing the optimal set of design parameters. The filter inductor so chosen must be of an appropriate size to satisfy this requirement of CCM and BW constraint, as stated in section 3.2. High inductance values also result in larger overall converter dimensions and more losses. Therefore, choosing the best value for the filter inductor is crucial. In light of this parameter, it is clear from table 3.4 that the ALO, FFA, and SSA in the swarm intelligence category provide the favorable outcomes conceivable within a reasonable range. The AEFA and AOA algorithms, as well as the rest of the physics-based algorithms, exhibit similar proficiency. It is to be observed that merely obtaining the minimized power loss values with minimum standard deviation is not sufficient to arrive at the best choice of the converter design parameters, as the design constraints also play a vital role in the choice of the converter specifications in terms of filter inductance, filter capacitance and operating frequency.

So far, the optimization approaches have been assessed based on their performance in convergence to the optimal solution while minimizing the total power loss in the operation of the dc-dc converter and obtaining the desired design of the circuit parameters which meets the CCM and BW constraints of each converters. It has been observed that a single strategy has not emerged which

performs better for every one of criteria at the same time. Under such a scenario, it is difficult to suggest an overall best algorithm that optimally solves the design optimization problem at hand the best and as such cannot be ascertained with absolute certainty. The top five best performing methods that provide us with satisfactory optimized results and are performing better when compared to the other algorithms within their categories are the WOA,SSA, BB-BC,MVO and GA algorithms. As a consequence, when the performance of the optimization techniques is compared overall, it is discovered that all approaches perform similarly except FFA and AEFA, which fails to find the optimized minimum power loss.

The amount of time it takes one algorithm to run 100 iterations is another success criteria in performance evaluation. The " tic-toc" function in MATLAB [91] was used to calculate the iteration time. The number of iterations in this study is set at 100. The iteration time data for each method is listed in Table 3.3. The SSA and WOA within the swarm intelligence based techniques have the shortest iteration periods when compared to the other ways in the design process. However, it is to be noted that although an algorithm with demonstrated improved performance on the basis of minimum iteration time, the rate of convergence of such an algorithm may be better than WOA and SSA compared to other algorithms. For the physics based algorithms, the BB-BC and MVO outperform the rest of the algorithms while GA performs better than AOA and TLBO. Under such a scenario, the algorithm with the minimal standard deviation can be said to be performing better statistically as well as being robust in attaining the optimal solution.

## 3.5 DC-DC Boost converter optimal design based MPPT tracking of standalone PV systems

Working performance of a PV module or array is largely reliant on external climatic conditions (temperature/irradiance) and is also non-linear in nature. To attempt harnessing the maximum solar energy utility, deployment of MPPT is inevitable [216]. MPPT uses a control algorithm to maximize power transmission in a manner to configure the DC-DC converter interface between the PV module and the load such that their respective impedances are equal [51] (figure 3.4).

It has been observed that a wide variation in reference PV module and

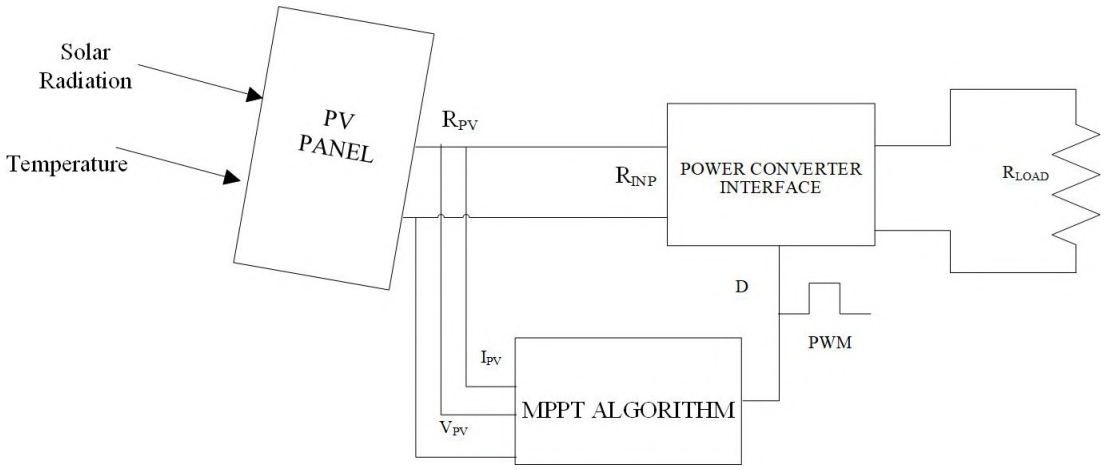


**Figure. 3.4:** Standalone PV system with MPPT connected to a load

algorithms exist in the literature where the focus has been on the pursuit of fast responsive and accurate tracking algorithms for MPPT. There is a requirement to evaluate the same reference PV module in combination with a suitable tracking algorithms and optimum power converter. This study encompasses evaluating well-known MPPT algorithms based on P&O, ANN, FLC, CS and PSO on a 120 Wp standalone PV system with a optimally configured dc-dc boost converter working as MPPT power interface. The overall schematic of the work is presented in figure 3.5.

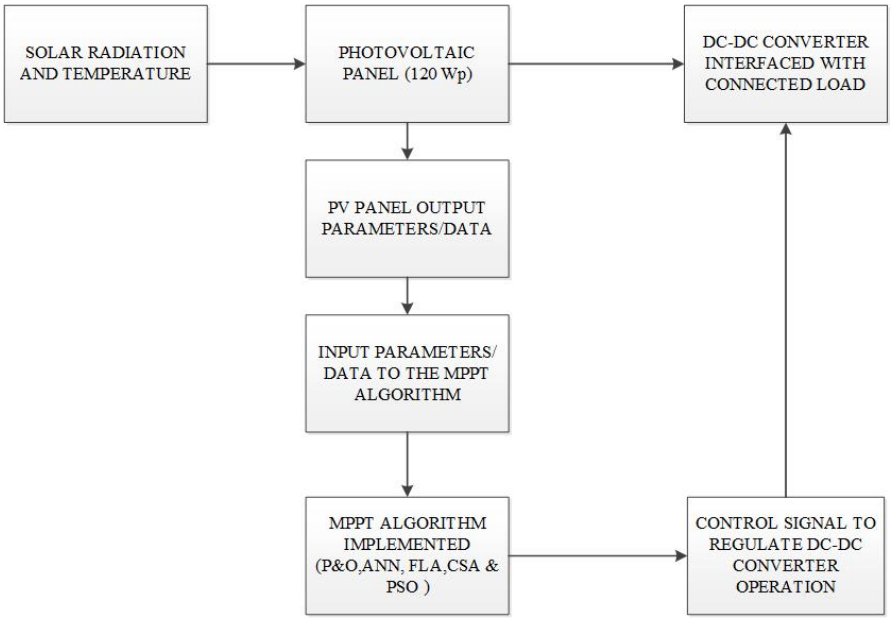


**Figure. 3.5:** Schematic of PV system integrated with DC-DC Converter and MPPT algorithm

The methodology followed in the current study covers the PV system modeling, DC-DC boost converter operation, and the MPPT algorithms. The

system modeling and simulation carried out along with the findings of comparative analysis is also reported with the results of simulation.

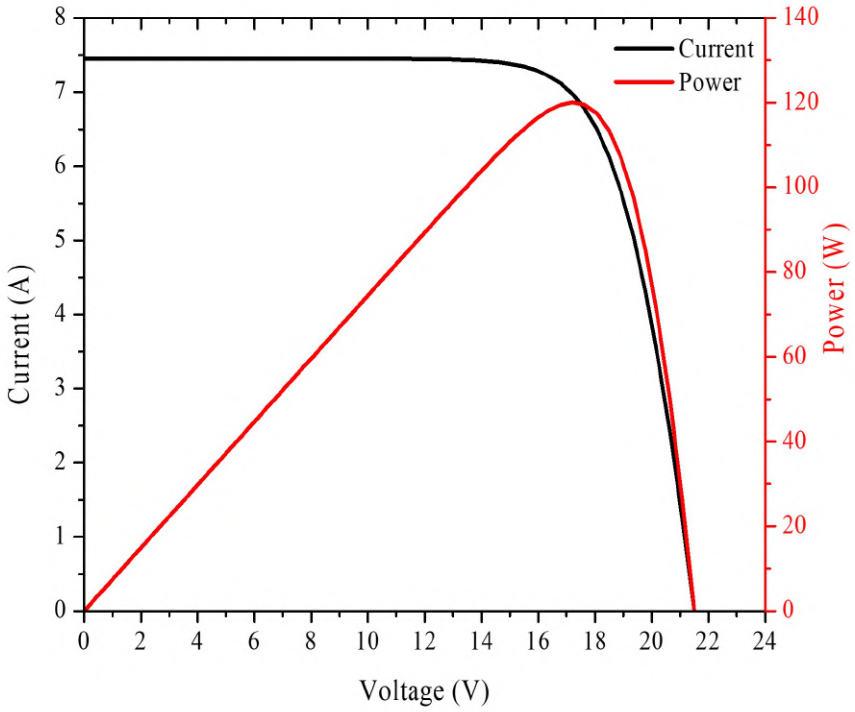


**Figure. 3.6:** I-V and P-V curve of the PV module at 1 $kW/m^2$ and 25 °C

The Kyocera KC-120-1 PV module is taken as a reference in this paper and its model in the software platform is implemented in MATLAB/SIMULINK as presented in detail in [28]. The model developed closely matches the electrical specification provided by the manufacturer's data-sheet as seen in Figure 3.6. Boost converters are used to make the output voltage higher than the input voltage. Input and output voltages and currents are connected to the duty ratio of the boost converter given by,

$$\frac{v_{in}}{v_{out}} = (1 - D) = \frac{i_{out}}{i_{in}} \tag{3.22}$$

### 3.5.1 Optimal Design of the DC-DC Boost Converter for MPPT tracking of standalone PV systems

Table 3.5 shows the variation of the parameters of the reference PV module Kyocera KC-120-1 under varying irradiance profiles. The PV module MPPT parameters have been listed under the three states of irradiance as well as the average

**Table 3.5:** Variation of Parameters of Kyocera KC-120-1 module under changing irradiance scenarios

| Sl no | Parameter | Value | | | |
|---|---|---|---|---|---|
| 1 | Irradiance ($W/m^2$) | 600 | 800 | 1000 | Average |
| 2 | $P_{pv}$ (MPPT) (W) | 71.69 | 96.014 | 120 | 98.90 |
| 3 | $V_{pv}$ (Mppt) (V) | 17.2 | 17.2 | 17.2 | 17.2 |
| 4 | $I_{pv}$ (Mppt) (A) | 4.1684 | 5.582 | 6.9781 | 5.576 |
| 5 | $R_{in}$ (MPPT) ($\Omega$) | 4.1262 | 3.0812 | 2.4648 | 3.224 |

values. The variation in the input impedance $R_{in}$ is taken as reference to calculate the range of the Duty ratio for the PV system connected with the 10 $\Omega$ load in the current study. The relation between $R_{in}$ and $R_L$ for a DC-DC boost converter is given by [28]:

$$R_{in} = R_L \times \left(1 - D^2\right) \tag{3.23}$$

The input values for the design optimization are taken to match the reference PV module. The input voltage is considered to be 21.5 V, where the rest of the parameters are selected from the table 3.2. Current and voltage ripple of $1 \times 10^{-2}$ A and 0.2 V respectively were considered as constraints for selecting the converter inductance and capacitance values. Equation (3.23) is used for selecting the range of duty ratio to be taken as a decision variable for the optimal design of the converter topology such that $0.35 \leq D < 0.5$ [244]. The methodology adopted in Section 3.4 is also adopted here for solving the design optimization problem of the DC-DC boost converter for MPPT application in standalone PV systems. Since the WOA and GWO gave comparable results for the optimization of the DC-DC converter in section 3.4 to optimize the boost converter for MPPT applications, they are considered assuming that the efficacy and performance of the algorithms do not change. Table 3.6 present the parameters of the optimally designed converter obtained using GWO and WOA.

**Table 3.6:** Optimal design parameters of the Boost converter for MPPT applications in Standalone PV systems given by GWO and WOA algorithms

| Optimization Algorithm | L (mH) | C ($\mu$F) | Fs (kHz) | $P_{BOOST}$(W) | $\eta$(%) |
|---|---|---|---|---|---|
| GWO | 10 | 92.58 | 100 | 7.04505 | 94.37 |
| WOA | 10 | 95.07 | 100 | 7.04505 | 94.37 |

The optimized value for the inductor sizing is equal to 10 mH while capacitor size close to 100 $\mu$F, these values are considered to be the optimal values. The

**Table 3.7:** Optimal Design of the Boost DC-DC converter for MPPT applications in Standalone PV systems

| Parameter | Value |
|---|---|
| Filter Inductor (L) | 10 mH |
| Filter Capacitance (C) | 100 $\mu$F |
| Switching Frequency ($F_s$) | 100 kHz |
| Optimal Duty Ratio ($D_{optimal}$) | 0.36 |

parameters of the optimized DC-DC boost converter for the MPPT application in PV systems are listed in table 3.7. These results are then utilized in section 3.5.2 for the MPPT tracking application involving standalone PV systems.

### 3.5.2 MPPT tracking of PV standalone system using optimized DC-DC Converter

The choice of the MPP tracking algorithms in this study is based on two things as reported in literature, the requirement of minimum sensing parameters for computation purpose and the ease of implementation for achieving MPPT keeping the tracking response as fast and accurate as possible. The current study implements five popular MPP tracking schemes reported in literature (as discussed in Chapter 2, section 2.4.2) to make a comparative investigation of their performance to external atmospheric perturbations. To minimize repetition of the established algorithms examined in this thesis, previous publications that extensively describe the underlying principles of P&O algorithm, FLA, ANN [28, 209] and [9, 93, 264] for the PSO and CS algorithm have been selected. Figure 3.7 shows the overall methodology of implementing the optimally designed boost converter for MPPT tracking with the five algorithms under consideration.

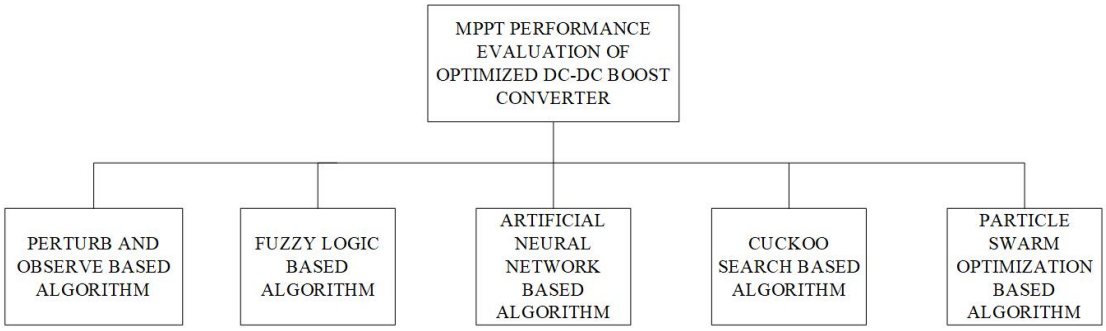


**Figure. 3.7:** Optimized Boost converter based MPPT tracking of PV systems using PSO, CSA, FLA, ANN and P&O techniques

In the work presented in this thesis, MATLAB/Simulink based models for

the PV system with MPPT schemes using the boost converter topology and the tracking algorithms are developed for the comparative assessment. Irradiance and ambient temperature are taken as inputs to the Simulink model and are saved to the workspace as array points having both time and irradiance data and time and temperature data respectively. The values of PV module power and MPPT tracked load power for each of the algorithms are recorded for each of these simulation scenarios and are presented here for analysis (as reported in[213]).

The effectiveness of tracking of any algorithm to match the MPP of the PV module under the varying profile of solar irradiance and temperature is evaluated using tracking efficiency which is defined as [28, 56]:

$$\eta = \frac{\int_0^t P_{inst}(t)dt}{\int_0^t P_{MPP}(t)dt} \tag{3.24}$$

Where $P_{inst}$ is the instantaneous power tracked by the algorithm and $P_{MPP}$ is instantaneous maximum power point of the PV module under the current conditions of solar irradiance and temperature [210]. The error in the tracking is also another parameter considered for comparative evaluation, defined as:

$$\%Error = (1 - \eta) \tag{3.25}$$

In addition to the above two parameters, average power output of the PV system (i.e. the average power tracked by each algorithm for each of the simulation periods), Relative Power Loss (RPL) and Relative Power Gain (RPG) [185] are also considered for performance evaluation of the algorithms.

The Relative Power Loss (RPL) and Relative Power Gain (RPG) of the MPPT technique can be calculated by [185]:

$$RPL = P_{TH} - P_{MPP} \tag{3.26}$$

$$RPG = \frac{P_{MPP,i} - P_{MPP,P\&O}}{P_{MPP,P\&O}} \times 100 \tag{3.27}$$

Where, $P_{TH}$ is the theoretical maximum power produced by the PV module at a given condition of Irradiance and Temperature, $P_{MPP}$ is the MPP tracked by the algorithm, $P_{mpp,i}$ is the MPP tracked by either ANN or FLA, while $P_{mpp,P\&O}$ is the MPP tracked by the P&O algorithm. In this study we have considered the boost-P&O as the reference algorithm to compare the RPG with.

The PV-based MPPT system model is created in the current study using

MATLAB/Simulink with five algorithms and the optimized DC-DC boost converter as the interface. The reference PV module (120 Wp, Kyocera KC-120-1 module) connected to a constant load emulated as a resistance of 10 Ω. The "ode45 (Dorman-Prince) solver" with configurable step size is used to run the simulation. From available literature [13, 87, 267] it has been noted that the temperature and irradiance profiles are chosen for a time range of 0.9 to 3.5 seconds. The temperature and irradiance profiles are also taken into consideration in the current study for a duration of 1 sec due to their uniformity and relevance. Accordingly, three scenarios are considered. Two with changing values of irradiance at fixed temperature and another at a fixed irradiance and temperature constitute the three profiles of the study as shown in figure 3.8. Figure 3.7 shows the overall methodology of implementing the optimally designed boost converter for MPPT tracking with the five algorithms under consideration.

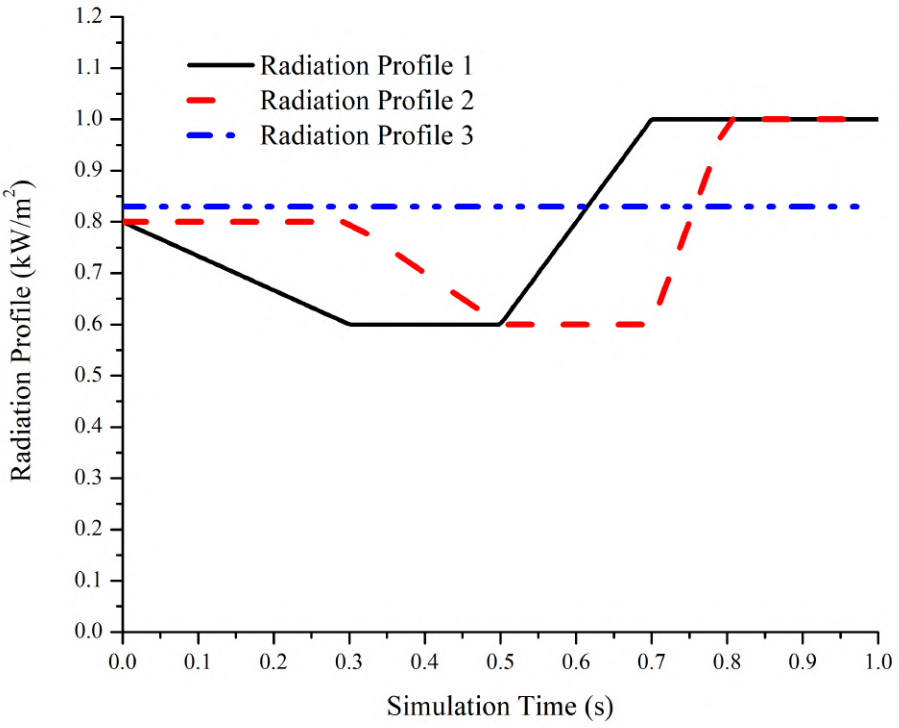


**Figure. 3.8:** Different set of irradiance profiles selected for analysis of MPPT algorithms

The variation in irradiance in the first scenario is gradual from 800 $W/m^2$ to 600 $W/m^2$ (0-0.3 sec) followed by a period of steady irradiance of 600 $W/m^2$. At time = 0.5 sec, the irradiance is increased with a constant slope to reach 1000 $W/m^2$ at 0.7 sec where it is held constant till the end of simulation time, i.e. 1 sec. In the second case of the considered profile, the irradiance has a steady starting

value of 800 $W/m^2$ and remains so till 0.3 seconds when it gradually decreases to 600 $W/m^2$ at 0.5 sec simulation time. It maintains the steady value till 0.7 sec when it increases gradually to reach 1000 $W/m^2$ in 0.8 sec simulation time and holds this value till the end of simulation time of 1 sec. For the third profile, the steady value of 830 $W/m^2$ is maintained for the entire duration of the simulation time of 1 sec. In all the three cases mentioned above, the value of temperature is kept at 28°C for uniformity.

Figures 3.9 to 3.11 highlight the changing PV module power over time, which results from the changing irradiance and temperature profile that it is being subject to, and the corresponding PV power being tracked by the algorithms. Each algorithm—P&O, FLA, ANN, CSA, and PSO—shows its MPPT being tracked. For a simulation time of 1 second, the variation of external atmospheric conditions and the consequent tracking reached by each algorithm clearly shows that the PSO has the best tracking performance, while the combination of P&O and ANN-based algorithm has the worst. For the boost converter the PSO controlled algorithm, followed by the CSA, the FLA, and finally the ANN algorithm and the P&O algorithm, achieves the greatest tracking. The PSO and CS algorithms are observed to adapt to changes in irradiance levels and monitor the accompanying changes more effectively. The performance of the ANN and P&O algorithms are quite similar however, close analysis shows that there is slow response to track the power change resulting in deviation from the desired operation point.

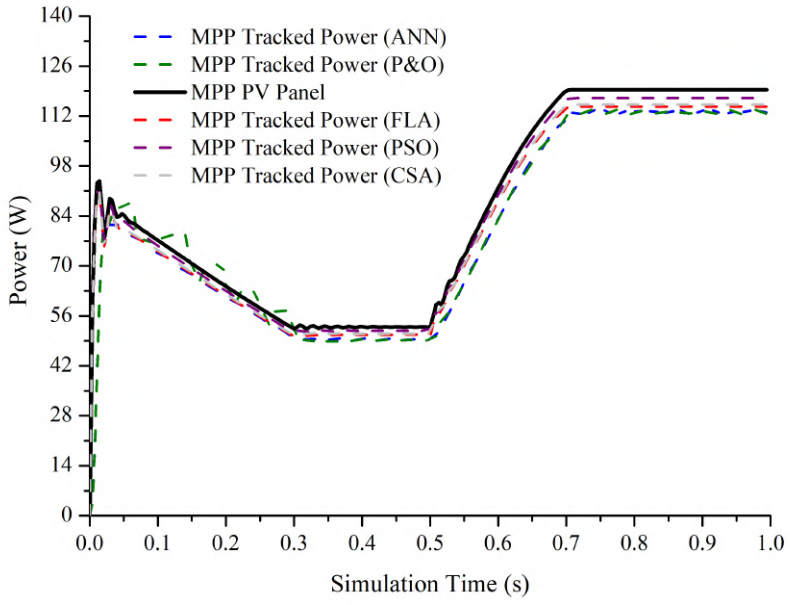


**Figure. 3.9:** MPPT tracked power for irradiance profile 1 using ANN, P&O, FLA, CSA and PSO based algorithms.

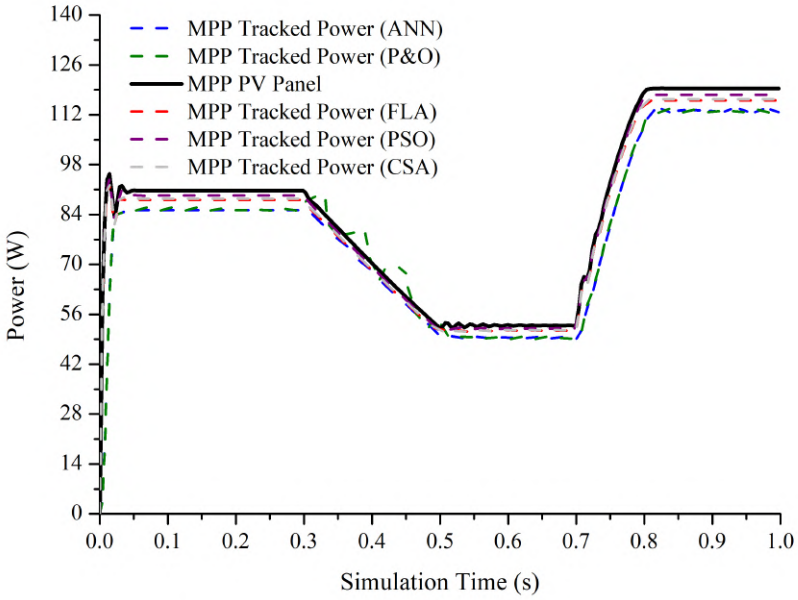


**Figure. 3.10:** MPPT tracked power for irradiance profile 2 using ANN, P&O, FLA, CSA and PSO based algorithms.

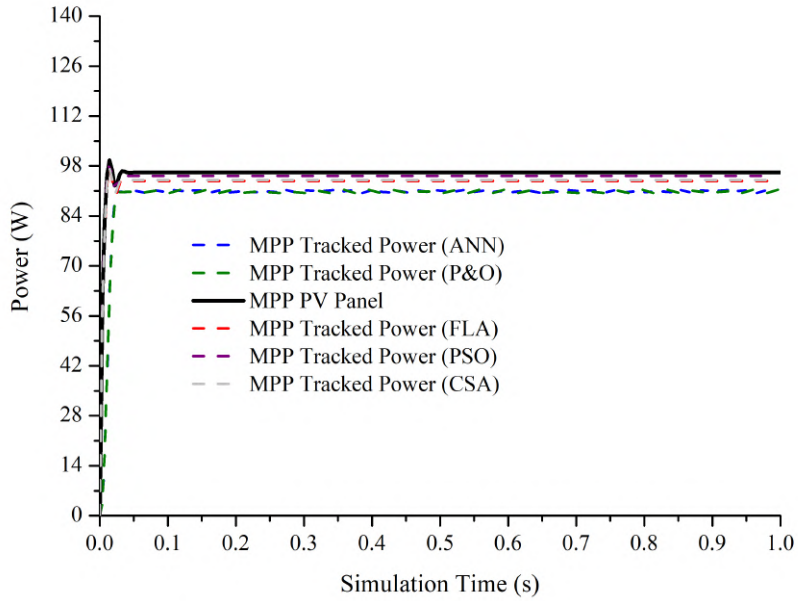


**Figure. 3.11:** MPPT tracked power for irradiance profile 3 using ANN, P&O, FLA, CSA and PSO based algorithms.

In order to track peak power operation, the PSO and CS based algorithm responds more dynamically and quickly by adjusting in response to the changing irradiance contour. While the changes in tracking profile of the PSO, CSA, FLA

and ANN in response to MPPT is gradual and avoids sudden transitions, the generated tracking profile for P&O algorithm has the most variation. Additionally, there is variation around the steady state operation as well as the regions of changes in irradiance profile. This is evident in the tracked power curves for the algorithm. This specifies that though the P&O algorithm is able to track the changing conditions and closely match the MPP, the oscillations lead to unstable operation and power loss as the switching conditions prevail in the boost converter as a result of the algorithms response to tracking the peak power point operation. This is clearly an unwanted scenario and corrective measures are needed to stabilize the system operation. Moreover, the switching transient also plays an important role in the operation of the converters as can be seen from the first peak to reach the maximum steady state indicated in figures 3.9 to 3.11.

**Table 3.8:** Tracking efficiency (%), Average Power Output , RPL, RPG and of the P&O, ANN, FLA, CSA and PSO based algorithms

| Irradiance Profile | Algorithm | Tracking Efficiency (%$\eta$) | Average Power Output of PV system (Pavg )(W) | Relative Power Loss (RPL) (W) | Relative Power Gain (RPG)(%) |
|---|---|---|---|---|---|
| Profile1 | P&O | 86 | 91.722 | 15.048 | 0 |
| | ANN | 89 | 95.03 | 11.74 | 3.6 |
| | FLA | 95.5 | 101.985 | 4.785 | 11.12 |
| | CSA | 96.5 | 103.0369 | 3.737 | 12.33 |
| | PSO | 97.5 | 104.114 | 2.66 | 13.51 |
| Profile 2 | P&O | 82.27 | 80.28 | 17.3 | 0 |
| | ANN | 87.56 | 85.44 | 12.135 | 6.43 |
| | FLA | 97.2 | 94.844 | 2.731 | 18.14 |
| | CSA | 97.5 | 95.135 | 2.44 | 18.50 |
| | PSO | 98.5 | 96.11 | 1.465 | 19.72 |
| Profile 3 | P&O | 93.29 | 89.24 | 6.415 | 0 |
| | ANN | 93.8 | 89.711 | 5.944 | 0.52 |
| | FLA | 97.5 | 93.263 | 2.392 | 4.5 |
| | CSA | 97.8 | 93.551 | 2.105 | 4.83 |
| | PSO | 98.99 | 94.698 | 0.957 | 6.12 |

Table 3.8 shows the average tracking efficiency, average PV system power output, Relative Power Loss (RPL), and Relative Power Gain (RPG) in tracking for the boost converter and algorithms combination based on simulation results. For the optimally designed boost converter, PSO has the maximum tracking efficiency (98.99%) and the lowest tracking error (approximately 1%) for the third scenario with constant irradiance and temperature profile. CSA tracks efficiently next (efficiency values of 96.5, 97.5 and 97.8). The FLA-based approach, emerges

as the third-best algorithm, performs similarly (% efficiency = 95.5, 97.2, and 97.5). ANN-based algorithm with tracking efficiency of 89, 87.56, and 93.8% follows FLA in tracking efficacy. P&O tracking yields 93.29% efficiency. P&O's steady state oscillations reduce boost converter efficiency. The PSO algorithm has the lowest tracking loss in the RPL at 1-3 W, followed by the CSA at 2-4 W and the FLA at 2.3-4.8 W while P&O loses equal 17.3 W. PSO again tops the other three algorithms in RPG with a maximum gain of 19.72%, followed by the CSA and FLA. PSO outperforms ANN, FLA, and CSA in tracking. With the boost converter, the PSO's power differential is within 6-19% of the base algorithm's reference power, i.e. the P&O-based MPPT algorithm. Thus, the boost converter with PSO outperforms the other algorithms in tracking efficiency, average power output, RPL, and RPG. Furthermore, it is seen that when compared with reported literature [3, 16, 28, 209] the tracking efficiency obtained in the current work shows improvement for the irradiance profiles by almost 4.5 to 5% respectively for changing irradiance profile to constant irradiance profile, which shows the effectiveness of the PSO algorithm.

## 3.6 Discussion

This study examines the effect of 23 metaheuristic algorithms' search efficacy on the solution of the optimized design of configuration of a DC-DC boost converters. The performance of the recently created AHA,ALO, BB-BC, DFA, HHO, SCA,SSA, FDA, EO, ASO, AEFA,ASA, MVO, MPA and AOA techniques is compared to that of the frequently used and established optimization techniques like ABC,GA, GWO,MFO,WOA, PSO,TLBO and FFA methods.

Within the swarm intelligence category, the three techniques WOA, SSA, and PSO in terms of iteration times, are quite comparable, although GA performs better in the other two categories. The DFA method is the most ineffective algorithm. DFA requires the most time to complete 100 iterations compared to other methods and has a higher computational complexity. The optimal fitness value that is attained for the boost converter for all the 23 algorithms is within the range of 1.7538 -1.7565 W. SSA demonstrates the quickest convergence in terms of minimum required iterations to reach the optimum value. It is followed by the WOA, SCA, and MFO methods respectively.

Despite the fact that the DFA technique yields satisfactory optimal results for the design optimization problem, the high computing cost necessitates

a lengthy iteration process. On the other hand, the GWO, MFO, PSO, WOA and FFA give good comparable performance, while the WOA outperforms all of the algorithms. DFA, ALO, ASO, and TLBO are the techniques with longest iteration time. And the FFA, AEFA, and TLBO stand out when examining the optimal values of the cost function. It should be emphasized at this point that the results could change if the fitness function is modified to include the duty ratio as another decision variable for the design optimization process, along with the range of filter inductor and capacitor values, minimal ripple content in current and voltage. Because of this, the final design parameters that achieve the goal of lowering overall power loss will also give rise to new optimized values. This will modify the total power loss estimates for the converter topology.

Taking into account all performance parameters, including the mean values, best value and highest value, iteration time, design constraints values for filter inductor and capacitor, switching frequency, computational time, best optimized result for minimized power loss, and convergence curve, the WOA in the swarm intelligence category outperforms the 22 other algorithms.

The optimized boost converter and five prominent algorithms used in PV-based MPPT tracking systems—P&O, FLA, ANN, CSA, and PSO have been compared for their tracking efficiencies. The PV system with an MPPT algorithm performs best when the load and dc-dc converter interface are properly selected. The boost converter with PSO with an overall tracking efficiency of 98.33%, and the tracking error being limited to about 1%, gives the best output performance with respect to tracking for the considered combination of converter interface and algorithm for PV based MPPT systems. This is closely followed by the performance of the CSA (% efficiency 97.267%), FLA based algorithm (% efficiency = 96.7%) and that of the ANN algorithm (% efficiency = 90.12%). The P&O based algorithm is the least effective in the tracking of the power for the scenarios considered and the steady state oscillations in P&O make it less efficient in terms of switching transients and operation of the boost converter for MPP tracking. The lowest loss in tracking considering the RPL is the boost converter with the PSO, while the converter with P&O gives the lowest performance. This indicates that with the boost converter, the difference in power tracked by the PSO is within 5% with respect to the reference power gained by the base algorithm, i.e. the P&O based MPPT.

The current work assesses the five most popular tracking algorithms in light of recent research on PV-based MPPT tracking for quick, rapid reaction to external disturbances and steady-state functioning. The limitation of the pre-

sented work lies in the hardware implementation and validation, which is still to be assessed. Furthermore, the results are taken at a simulated load of fixed value. The potential of load change exists in real-world applications; thus, it is necessary to implement such conditions to better understand how the system performs under dynamic load-changing circumstances. This brings up the possibility of further research and is worth considering. In any case, the current study should serve as a guide for determining the ideal boost converter architecture and tracking algorithm for standalone PV-based MPPT systems.

## 3.7 Summary

In this chapter, the problem of design optimization of a DC-DC boost converter is presented. Within the bounds of constraints, optimal results for the minimized converter loss obtained for the boost converter was 1.7538 W. The study also analyzed and evaluated 23 metaheuristic techniques that optimize the design of the dc-dc converter to reduce internal power loss. The SCA, DFA, AHA, ASO, EO, FDA, and AOA procedures are among the 23 that haven't been previously applied for the design optimization process. When the minimal iteration time and standard deviation were taken into account, the WOA, SSA, SCA, and MFO techniques among the swarm intelligence based algorithms showed comparable results based on convergence rate.

The problem of designing an optimal DC-DC boost converter for MPPT application in standalone PV systems is presented next. The optimized DC-DC boost converter in combination with the PSO algorithm outperforms all other compared algorithms based on tracking efficiency (up to 98.3 %), RPL and RPG. The combinations of boost converter and CSA, boost-FLA and boost-ANN all give better results when compared with the combination of boost-P&O algorithm. The optimization algorithms used in the current study for boost converter optimal design can be employed with the goal of improving MPP tracking performance in future research endeavors.